JOURNAL OF SOLID STATE CHEMISTRY 119, 8–12 (1995)

# Crystal Structure of $(Mo,W)_9O_{25}$, Homologue of the $Mo_4O_{11}$ (Orthorhombic)-Type Structure

O. G. D'Yachenko,* V. V. Tabachenko,* and M. Sundberg†

*X-Ray Laboratory, Chemical Department, Moscow State University, 119899 Moscow, Russia; and †Department of Inorganic Chemistry, Arrhenius Laboratory, Stockholm University, S-10691 Stockholm, Sweden

Received December 16, 1993; in revised form March 6, 1995; accepted March 8, 1995

**The structure of $Mo_{7.6}W_{1.4}O_{25}$ has been determined from single crystal X-ray data. The symmetry is monoclinic with lattice parameters $a = 5.448(1)$, $b = 27.639(8)$, $c = 6.739(1)$ Å, $\beta = 90.180(9)°$, and space group $P2_1/n$. The refinement led to $R = 0.046$ for 2060 observed unique reflections. The Mo : W ratio was confirmed by microanalysis. The $(Mo, W)_9O_{25}$ structure is built up of corner-sharing distorted $MO_6$ octahedra in slabs of $ReO_3$-type, cut parallel to {211} and seven octahedra wide along two subcell axes. The slabs appear alternatively in mirrored orientations. The slabs are mutually linked by corner sharing of fairly regular $MoO_4$ tetrahedra so that five-sided tunnels are formed. The $(Mo,W)_9O_{25}$ structure is related to the orthorhombic modification of $Mo_4O_{11}$ and can be considered as the second member ($m = 7$) of the homologous series with the general formula $M_{m+2}O_{3m+4}$. High-resolution electron microscopy images showed well-ordered crystal fragments.** © 1995 Academic Press, Inc.

## INTRODUCTION

Molybdenum and tungsten form many binary and ternary mixed valency metal oxides, with complex stoichiometries and crystal structures. For slightly reduced compounds, $MO_{3-x}$ ($0 < x < 0.13$), two homologous series of phases, $M_nO_{3n-1}$ and $M_nO_{3n-2}$, have been reported (1). The first series comprises the {102} crystallographic shear (*CS*) structures, observed both in the binary and the ternary systems, while the latter one consists of the {103} *CS* structures formed for $WO_{3-x}$ with $0.08 < x < 0.13$. Many $(Mo,W)O_{3-x}$ structures with $x > 0.13$ consist of a framework of metal oxygen polyhedra, which share corners or edges so that 3-, 4-, 5-, or 6-sided tunnels are formed.

During the last decade there has been a great interest in the physical properties of molybdenum and tungsten oxides, particularly in relation to their electrical conductivity, magnetic susceptibility, and phase transitions at low temperature (2–5). The influence of deviations from the stoichiometric composition on the physical properties has also been studied (6).

In an investigation aiming at clarifying the formation conditions of phases in the $UO_2$–$MoO_2$–$MoO_3$–$WO_3$–$H_2O$ system, single crystals of a new (Mo,*W*) oxide were obtained by hydrothermal synthesis. These crystals have been examined by single crystal X-ray diffraction and high-resolution electron microscopy (HREM). The results are presented below.

## EXPERIMENTAL

A multiphasic sample was obtained by heating a mixture of $UO_2 : MoO_2 : MoO_3 : WO_3$ equal to 1 : 1 : 6 : 2 in a Teflon tube, filled with water to three-fourths of its volume and closed by a Teflon screw, at 573 K and $P = 500$ bar for two weeks. Dark-blue to dark-brown pillar-shaped crystals were selected for investigation.

A small parallelepiped (dark blue in color) was cut, mounted, and investigated on an Enraf–Nonius CAD4 diffractometer with monochromatized Mo$K\alpha$ radiation. Unit cell dimensions were refined from 24 reflections in the range $36° < 2\theta < 37.5°$. The $\Omega$–$\theta$ technique was used for data collection. The single crystal X-ray data were corrected for Lorentz, polarization, and absorption effects. Further details about the experimental conditions are given in Table 1.

The examined single crystal and three additional selected crystals were analyzed with a "CAMEBAX—microbeam" electron microprobe. Single crystals of $UMo_{10}O_{32}$ and $WO_3$ were used as standards. Atomic percentages were determined at 6–10 points on each crystal, using the $M_\alpha$-line of uranium and $L_\alpha$-lines of the two other cations. The MBX COR program (ZAF—correction) was applied in the calculations.

Selected crystals were crushed in an agate mortar, dispersed in *n*-butanol, and drops of the resultant suspension were put on a holey carbon film supported by a Cu grid. HREM images were recorded in a JEOL 200CX electron microscope equipped with a top-entry goniometer stage (max. tilt ±10°). The radius of the objective aperture used corresponded to 0.41 $Å^{-1}$ in reciprocal space. Theoretical



0022-4596/95 $12.00

TABLE 1
**Experimental Conditions for the Crystal Structure Determination of $Mo_{7.6}W_{1.4}O_{25}$**

| | |
|---|---|
| Unit cell dimensions | $a$ = 5.448 (1) Å, $b$ = 27.639 (8) Å, $c$ = 6.739 (1) Å, $\beta$ = 90.180 (9)° |
| Unit cell volume | 1014.8 Å$^3$ |
| Space group | $P2_1/n$ |
| Formula units per unit cell, $Z$ | 2 |
| Calculated density, $D_x$ | 4.536 g cm$^{-3}$ |
| Crystal size, mm | 0.02 × 0.03 × 0.09 |
| **Intensity data collection** | |
| λ Å | 0.7107 |
| Maximum sin $\theta/\lambda$ | 0.7448 |
| Range of $h$, $k$, $l$ | −8–8, 0–41, 0–10 |
| Number of collected reflections | 3577 |
| Number of unique reflections | 2990 |
| Number of observed reflections | 2060 |
| Criterion of significance | $I > 3\sigma(I)$ |
| Absorption correction | $\psi$-scan + DIFABS |
| Linear absorption coefficient | 130.3 cm$^{-1}$ |
| Extinction coefficient | 2.37(4) × 10$^{-7}$ |
| **Structure refinement** | |
| Minimization of | $w\,\Delta F^2$ |
| Number of refined parameters | 68 |
| Weighting scheme | unity |
| Final $R$ for observed reflections | 0.046 |
| Final $R_w$ for observed reflections | 0.046 |

images were calculated using a local version of the multislice program suite SHRLI (7). A JEOL 2000FX II electron microscope equipped with a LINK QX200 X-ray analysis system was used to study the fragments by electron diffraction in combination with energy dispersive spectroscopy (EDS) analysis.

## X-RAY DIFFRACTION STUDIES

Analysis of the reflections with intensity $I > 3\sigma(I)$ showed systematic absences satisfying the conditions of space group $P2_1/n$. Moreover, a comparison of the intensity of 591 reflection pairs ($hkl$ and $\bar{h}kl$), which would be equivalent in the case of orthorhombic symmetry, revealed 47 pairs with a deviation of more than $3\sigma(I)$ and 13 pairs with a deviation of more than $5\sigma(I)$. This fact supports the choice of monoclinic symmetry. It was not possible to confirm the monoclinic symmetry by refinement of the lattice parameters from an X-ray powder pattern of the multiphasic bulk specimen, as the dark-blue and dark-brown pillar-like crystals were in the minority. However, an almost single-phased but microcrystalline sample of the $(Mo,W)_9O_{25}$ compound has recently been prepared by conventional high-temperature synthesis (8). Refinement of the unit cell parameters from an X-ray powder pattern confirmed the monoclinic unit cell. The obtained lattice parameters $a$ = 5.4453(6), $b$ = 27.632(5), $c$ = 6.7376(7) Å, and $\beta$ = 90.17(2)° are very close to those presented in Table 1.

The crystal structure was determined by direct methods. The structural refinements were carried out by means of the CAD4-SDP package, with atomic scattering factors from International Tables for X-Ray Crystallography (9). Extinction correction, included in the SDP package, was made by using the formula $|F_c| = |F_o|(1 + gI_c)$, where $I_c$ is the calculated intensity and $g$ is the secondary extinction coefficient. The final atomic parameters and temperature factors are given in Table 2. The composition $Mo_{7.6}W_{1.4}O_{25}$ of the investigated crystal was obtained from refinement of the occupancy factors of the metal atom positions.

The electron microprobe analysis of the examined single crystal and three additional selected crystals, all with unit cell dimensions within the range $a$ = 5.431–5.449 Å, $b$ = 27.584–27.651 Å, $c$ = 6.716–6.740 Å, and $\beta$ = 90.14–90.20° showed an absence of uranium atoms in all four crystals, as no signal from uranium was observed. The average cation ratio, Mo : W, of the crystal used in the single-crystal X-ray investigation was found to be 21.5(6) : 3.8(1), corresponding to the formula $Mo_{7.55(8)}W_{1.45(8)}O_{25}$. The analysis thus confirmed the composition $Mo_{7.6}W_{1.4}O_{25}$ obtained from the structure refinement. Further analysis of the other three crystals indicated that the Mo content was slightly higher in the brown-colored crystals, $Mo_{7.90(2)}W_{1.10(2)}O_{25}$, than in the dark-blue one, $Mo_{7.23(8)}W_{1.77(8)}O_{25}$. A black crystal with a much higher tungsten content $Mo_{4.62(9)}W_{4.38(9)}O_{25}$ was also observed.

## ELECTRON MICROSCOPY STUDY

Three different structure types were identified from electron diffraction (ED) patterns of thin crystal fragments, namely, {102} *CS* structures, "$UMo_{10}O_{32}$," and the present phase $M_9O_{25}$ ($M$ = Mo,W). Most ED patterns taken of the latter phase showed sharp reflections. Two examples are shown in Fig. 1. No streaking of the spots was observed, which indicates that the examined crystal fragments were well-ordered. It is noteworthy that no ED pattern of an $(Mo,W)_4O_{11}$ phase has so far been recorded from this sample.

The HREM image in Fig. 2 shows a well-ordered structure. The image is recorded with the [101] direction parallel to the electron beam, instead of [100], which is normally used. This is due to the limitation in crystal tilt and the preferred orientation of the examined fragments. However, all three orientations, [100], [001], and [101], can be used to study the variation in the width of $ReO_3$-type slabs. So far, no deviation in the width of the slabs has been observed. Theoretical images were calculated using the parameters given in Table 2. There is good agreement between the recorded HREM image and the

TABLE 2
Final Atomic Coordinates and Anisotropic Temperature Factors (Å$^2$) with e.s.d's in Parentheses for $Mo_{7.6}W_{1.4}O_{25}$

| | Fraction Mo | $x$ | $y$ | $z$ | $U_{11}$ | $U_{22}$ | $U_{33}$ | $U_{12}$ | $U_{13}$ | $U_{23}$ |
|---|---|---|---|---|---|---|---|---|---|---|
| *M1* | 1.0 | −0.0125(2) | 0.21029(3) | 0.7059(5) | .0062(4) | .0031(3) | .0043(4) | .0008(3) | −.0003(3) | .0006(3) |
| *M2* | 0.554(8) | 0.5033(1) | 0.15876(2) | 0.0306(1) | .0042(2) | .0042(2) | .0042(2) | .0001(2) | −.0001(2) | −.0002(2) |
| *M3* | 0.821(7) | −0.0036(1) | 0.10488(3) | 0.3563(1) | .0039(3) | .0055(3) | .0041(3) | −.0001(3) | −.0002(2) | .0012(2) |
| *M4* | 0.909(6) | 0.5005(2) | 0.05103(3) | 0.6805(1) | .0037(3) | .0046(3) | .0043(3) | .0001(3) | .0001(3) | −.0008(3) |
| *M5* | 1.0 | 0 | 0 | 0 | .0052(5) | .0092(5) | .0077(5) | −.0003(3) | −.0002(5) | .0023(5) |
| O1 | | 0.502(2) | 0.3255(3) | −0.010(1) | 1.6(2)[a] | | | | | |
| O2 | | 0.006(2) | 0.2736(3) | 0.653(1) | 1.6(2)[a] | | | | | |
| O3 | | −0.004(2) | 0.3881(3) | 0.355(1) | 1.5(2)[a] | | | | | |
| O4 | | 0.503(2) | 0.4424(3) | 0.679(1) | 0.8(1)[a] | | | | | |
| O5 | | ½ | 0 | ½ | 0.4(2)[a] | | | | | |
| O6 | | 0.220(2) | 0.1950(4) | 0.872(6) | 1.8(2)[a] | | | | | |
| O7 | | 0.201(2) | 0.2999(4) | 0.318(1) | 1.8(2)[a] | | | | | |
| O8 | | 0.280(2) | 0.1383(4) | 0.195(1) | 1.6(2)[a] | | | | | |
| O9 | | 0.274(2) | 0.3563(3) | 0.659(1) | 1.0(1)[a] | | | | | |
| O10 | | 0.231(2) | 0.4124(3) | −0.000(1) | 1.1(1)[a] | | | | | |
| O11 | | 0.227(2) | 0.0829(3) | 0.521(1) | 1.0(1)[a] | | | | | |
| O12 | | 0.264(2) | 0.4706(3) | 0.325(1) | 1.0(1)[a] | | | | | |
| O13 | | 0.266(3) | 0.0264(3) | 0.844(1) | 0.9(1)[a] | | | | | |

*Note.* The temperature factor expression is $\exp[-2\pi^2(U_{11}h^2a^{*2} + U_{22}k^2b^{*2} + U_{33}l^2c^{*2} + 2U_{12}hka^*b^* \cos\gamma^* + 2U_{13}hla^*c^* \cos\beta^* + 2U_{23}klb^*c^* \cos\alpha^*)]$.

[a] Atoms were refined isotropically and the values given correspond to the $B_{iso}$.

simulated one inserted in Fig. 2, which verifies the structure.

Convergent beam electron diffraction could not be used to confirm the small deviation from orthorhombic symmetry ($\beta \approx 90.18°$), as no suitable crystal fragments were found.

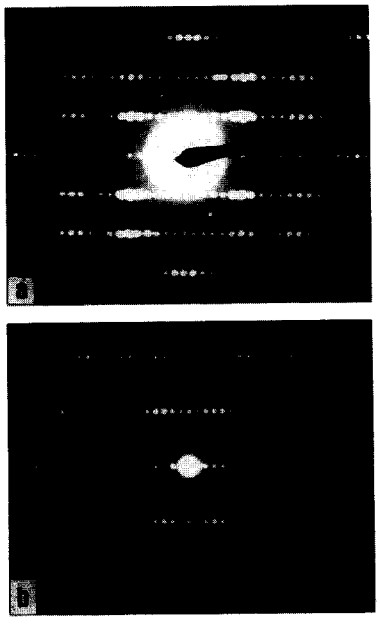

FIG. 1. Electron diffraction patterns of a thin crystal fragment, $(Mo,W)_9O_{25}$: (a) [100] zone and (b) [101] zone.

EDS analysis of a few crystallites giving ED patterns as in Fig. 1 indicated a composition of $Mo_{\approx 7.1}W_{\approx 1.9}O_{25}$, which is fairly close to $Mo_{7.6}W_{1.4}O_{25}$ previously obtained from the X-ray study. The analysis also showed that uranium was not present in the examined $(Mo,W)_9O_{25}$ crystal fragments.

## DISCUSSION

The structure of $Mo_{7.6}W_{1.4}O_{25}$, shown in Fig. 3, is built up of a network of corner-sharing $MO_6$ octahedra that

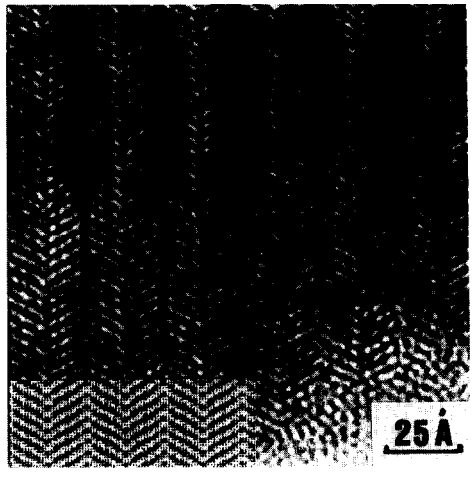


FIG. 2. HREM image of a thin crystal fragment, $(Mo,W)_9O_{25}$ ([101] projection), with the simulated image inserted in the lower left corner. Crystal thickness, 17.3 Å; defocus value, −200 Å

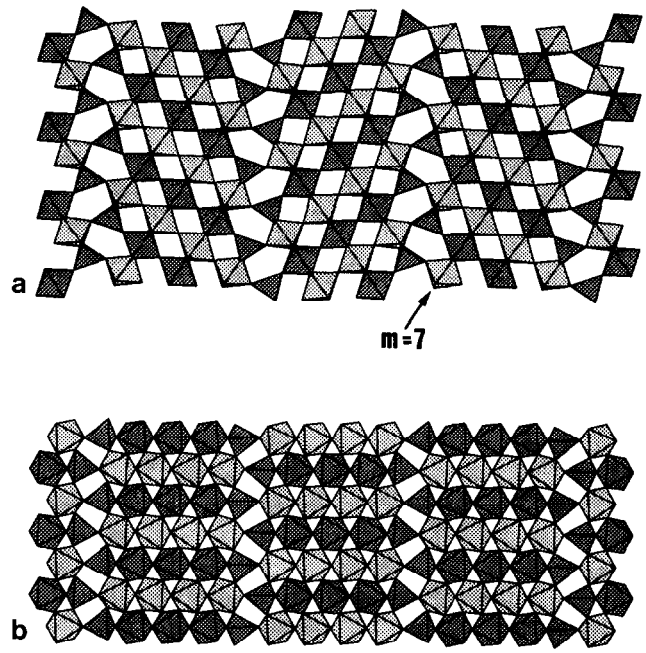


FIG. 3. The crystal structure of $Mo_{7.6}W_{1.4}O_{25}$ projected along (a) [100] and (b) [001]. The $M$ atoms in the octahedra are located at $x \approx 0$ and $x = 0.5$. The corresponding $MO_6$ octahedra are marked with different shades of grey.

TABLE 3
Selected Interatomic Distances (Å) in $Mo_{7.6}W_{1.4}O_{25}$

| | | | |
|---|---|---|---|
| $M_1$–O6 | 1.738(10) | $M_2$–O8 | 1.742(10) |
| $M_1$–O7 | 1.760(10) | $M_2$–O3 | 1.757(9) |
| $M_1$–O1 | 1.761(10) | $M_2$–O9 | 1.759(9) |
| $M_1$–O2 | 1.790(10) | $M_2$–O2 | 2.043(10) |
| Average | 1.762 | $M_2$–O6 | 2.126(10) |
| | | $M_2$–O7 | 2.126(10) |
| | | Average | 1.926 |
| $M_3$–O4 | 1.771(8) | $M_4$–O13 | 1.824(9) |
| $M_3$–O11 | 1.782(9) | $M_4$–O12 | 1.835(9) |
| $M_3$–O10 | 1.807(9) | $M_4$–O5 | 1.8631(8) |
| $M_3$–O9 | 2.091(10) | $M_4$–O10 | 2.023(9) |
| $M_3$–O8 | 2.105(10) | $M_4$–O11 | 2.034(9) |
| $M_3$–O1 | 2.125(10) | $M_4$–O3 | 2.052(9) |
| Average | 1.947 | Average | 1.938 |
| $M_5$–O12 (×2) | 1.920(9) | | |
| $M_5$–O13 (×2) | 1.933(9) | | |
| $M_5$–O4 (×2) | 1.999(8) | | |
| Average | 1.951 | | |

*Note.* Standard deviations are in parentheses. $M_1$ and $M_5$ = Mo; $M_2$, $M_3$, and $M_4$ = Mo,W.

form slabs of $ReO_3$ type. The slabs are seven octahedra wide along two of the subcell axes and cut parallel to {211} of the basic $ReO_3$ cell. The slabs appear alternatively in mirrored orientations. They are mutually connected through corner-sharing of $MO_4$ tetrahedra, so that five-sided tunnels are formed. The structure is related to that of the previously reported $Mo_4O_{11}$ (o-rh) (10–12).

The metal–oxygen bond distances are given in Table 3. The table shows that three of the five $M$ atoms ($M_2$, $M_3$, and $M_4$) coordinate six O atoms with three shorter and three longer $M$–O distances, thus forming three considerably distorted $MO_6$ octahedra. The average $M$–O bond distances of these metal atoms are in the range 1.926–1.947 Å. The distortion can be considered to arise essentially from displacement of the metal atom from the center toward one of the faces of the octahedron. The three positions mentioned are occupied by Mo and W atoms (see Table 2). The most distorted octahedron is that of $M_2$, situated at the edge of the slab.

The $M_5$ position is occupied exclusively by Mo atoms with Mo–O distances in the range 1.92–1.99 Å, giving an average Mo–O value of 1.951 Å. This octahedron is the most regular of all the octahedra and is located in the middle of the slab. Table 2 shows that the W content of the octahedra decreases toward the middle of the $ReO_3$-type slab, where the distortion of the octahedra is the least (see Table 3). The tetrahedrally coordinated $M_1$ position is occupied by Mo atoms exclusively, with Mo–O distances in the range 1.738–1.790 Å. Figure 3b shows that the $M_1$ atoms coordinate three O atoms of three adjacent $(Mo,W)O_6$ octahedra in one layer and one O atom of a fourth octahedron of another layer to form a fairly regular $MoO_4$ tetrahedron connecting the layers. There is also fairly good agreement between the $M$–O distances given for the $Mo_{7.6}W_{1.4}O_{25}$ structure above and those previously reported for the $Mo_4O_{11}$ (o-rh) structure (12), which has a similar distortion pattern. In the $Mo_4O_{11}$ (o-rh) structure three-fourths of the Mo atoms coordinate six O atoms to form three distorted $MoO_6$ octahedra, while the fourth Mo atom coordinates four O atoms in a fairly regular $MoO_4$ tetrahedron with Mo–O distances in the range 1.736–1.775 Å. The very slight deviation from orthorhombic symmetry ($\beta = 90.18°$) observed for the $Mo_{7.6}W_{1.4}O_{25}$ phase might be due to the W content and the accompanying coordination distortion, especially that of the $M_2$ octahedron.

The main difference between the $(Mo,W)_9O_{25}$ and the $Mo_4O_{11}$ (o-rh) structures is the width of the basic $ReO_3$-type slabs. In the $Mo_4O_{11}$ (o-rh) structure, there are six corner-sharing $MO_6$ octahedra along two of the basic subcell axes, while in the $(Mo,W)_9O_{25}$ structure there are seven octahedra. The latter structure can thus be regarded as the second member ($m = 7$) of a homologous series of phases based on the $Mo_4O_{11}$ (o-rh) structure ($m = 6$). The general formula is $M_{m+2}O_{3m+4}$, where the members differ in width of the slabs, expressed in terms of the number of octahedra, $m$. The possibility of such a homologous series of phases has previously been suggested (13), but

so far no representative has been observed in the Mo–O system.

However, homologues of the $Mo_4O_{11}$ (o-rh) structure have previously been reported for monophosphate tungsten bronzes with empty pentagonal tunnels (14). This family of structures was denoted as "$MPTB_P$" with the general formula given as $(PO_4)_2(WO_3)_m$. In these compounds, $PO_4$ tetrahedra connect the $ReO_3$-type slabs so that pentagonal tunnels are created.

Substitution of some W for Mo has previously been observed to increase the width of the $ReO_3$-type slabs. In the {102} *CS* structures, the homologous series $M_nO_{3n-1}$ is formed, where $n$ corresponds to the number of corner-sharing octahedra in the slab. The members $n = 8$ and $n = 9$ have been observed as binary molybdenum oxides (1), while for the ternary molybdenum–tungsten oxides the corresponding values are $n = 10$–$14$. Recently, HREM studies in combination with EDS analysis of complex oxides in the $UO_2$–$MoO_2$–$MoO_3$–$WO_3$ system have shown similar results: the width of the $ReO_3$-type slabs increases when W is substituted for Mo in the complex U–Mo oxides (15).

There exist two modifications of $Mo_4O_{11}$ composition which both give rise to homologous series of related phases with the general formula $M_{m+2}O_{3m+4}$ (13). One modification is the $Mo_4O_{11}$ (o-rh) phase described above, which is formed above ≈600°C. The other is the low-temperature modification, $Mo_4O_{11}$ (mon), obtained below ≈600°C (16). Both structures are built up of $ReO_3$-type slabs of equal width ($m = 6$), but the slabs are differently oriented. In $Mo_4O_{11}$ (mon) all slabs have the same orientation, while in $Mo_4O_{11}$ (o-rh) the slabs appear alternatively in mirrored orientations. In both structure types the slabs are mutually connected through $MoO_4$ tetrahedra. In the first phase, alternating four- and six-sided tunnels are formed, while in the latter phase only five-sided tunnels are created. The $(Mo,W)_9O_{25}$ structure discussed above adopts the high-temperature orthorhombic structure, although it is prepared at a low temperature, 300°C. This is probably due to the hydrothermal conditions used for the synthesis of the crystals. In a reduced specimen, $Mo_{0.72}W_{0.28}O_{3-x}$, prepared by soft chemistry, the homologues $m = 4,7$, and 8 of the $Mo_4O_{11}$(mon) type structure have been observed by HREM technique (17).

Recently, HREM studies of crystals from a $Mo_{7.3}W_{1.7}O_{25}$ sample, prepared by heating appropriate amounts of $MoO_2$, $MoO_3$, and $WO_3$ at 600–800°C, revealed both disorder of the $Mo_4O_{11}$ (o-rh)-type structure and mixed monoclinic–orthorhombic stacking (8).

## ACKNOWLEDGMENTS

The authors thank Professor L. Kihlborg and Professor L. M. Kovba for their kind interest in this work and for stimulating discussions. This work has partly been supported by the Swedish Natural Science Research Council.

## REFERENCES

1. A. Magnéli. *Acta Crystallogr.* **6,** 495 (1953).
2. W. Sahle and M. Nygren, *J. Solid State Chem.* **48,** 154 (1983).
3. H. Gruber, H. Haselmair, and H. P. Fritzer, *J. Solid State Chem.* **47,** 84 (1983).
4. H. Gruber, E. Krautz, H. P. Fritzer, K. Gatterer, and A. Popitsch, *Phys. Status Solidi A* **98,** 297 (1986).
5. H. Fujishita, M. Sato, S. Sato, and S. Hoshino, *J. Solid State Chem.* **66,** 40 (1987).
6. H. Gruber, H. P. Fritzer, and A. Popitsch, *Adv. Ceram.* **23,** 409 (1987).
7. M. A. O'Keefe, P. R. Buseck, and S. Iijima, *Nature (London)* **274,** 322 (1978).
8. L. Kihlborg, B.-O. Marinder, M. Sundberg, F. Portemer, and O. Ringaby, *J. Solid State Chem.* **111,** 111 (1994).
9. "International Tables for X-Ray Crystallography," Vol. IV, p. 72. Kynoch Press, Birmingham, UK, 1974.
10. A. Magnéli, *Acta Chem. Scand.* **2,** 861 (1948).
11. L. Kihlborg, *Arkiv. Kemi* **21,** 365 (1963).
12. S. Åsbrink and L. Kihlborg, *Acta Chem. Scand.* **18,** 1571 (1964).
13. L. Kihlborg, *Arkiv. Kemi* **21,** 471 (1963).
14. M. M. Borel, M. Goreaud, A. Grandin, P. Labbé, A. Leclaire, and B. Raveau, *Eur. J. Solid State Inorg. Chem.* **28,** 93 (1991).
15. M. Sundberg and V. Tabachenko, *Microsc. Microanal. Microstruct.* **1,** 373 (1990).
16. L. Kihlborg, *Acta Chem. Scand.* **13,** 954 (1959).
17. F. Portemer, M. Sundberg, L. Kihlborg, and M. Figlarz, *J. Solid State Chem.* **103,** 403 (1993).